

# Numerical dispersion compensation for Partial Coherence Interferometry and Optical Coherence Tomography

A. F. Fercher, C. K. Hitzenberger, M. Sticker, R. Zawadzki,\*

Institute of Medical Physics, University of Vienna, Waehring Str.13, A-1090 Wien

\*Physics Department, Nicholas Copernicus University, ul. Grudziadzka 5/7, PL-87-100 Torun  
[adolffriedrich.fercher@univie.ac.at](mailto:adolffriedrich.fercher@univie.ac.at)

B. Karamata and T. Lasser

Institut d'Optique Appliquée, EPFL, Ecublens, CH-1015 Lausanne

**Abstract:** Dispersive samples introduce a wavelength dependent phase distortion to the probe beam. This leads to a noticeable loss of depth resolution in high resolution OCT using broadband light sources. The standard technique to avoid this consequence is to balance the dispersion of the sample by arranging a dispersive material in the reference arm. However, the impact of dispersion is depth dependent. A corresponding depth dependent dispersion balancing technique is difficult to implement. Here we present a numerical dispersion compensation technique for Partial Coherence Interferometry (PCI) and Optical Coherence Tomography (OCT) based on numerical correlation of the depth scan signal with a depth variant kernel. It can be used *a posteriori* and provides depth dependent dispersion compensation. Examples of dispersion compensated depth scan signals obtained from microscope cover glasses are presented.

©2001 Optical Society of America

OCIS codes: 120.3180 Interferometry; 170.4500 Optical coherence tomography

---

## References and links

1. A.F. Fercher and E. Roth, "Ophthalmic laser interferometry," Proc. SPIE **658**, 48-51 (1986).
2. D. Huang, E.A. Swanson, C.P. Lin, J. S. Schuman, W.G. Stinson, W. Chang, M.R. Hee, T. Flotte, K. Gregory, C.A. Puliafito, J.G. Fujimoto, "Optical coherence tomography," Science **254**, 1178-1181 (1991).
3. A.F. Fercher, C. K. Hitzenberger, M. Sticker, E. Moreno-Barriuso, R. Leitgeb, W. Drexler, H. Sattmann, „A thermal light source technique for optical coherence tomography," Opt. Commun. **185**, 57-64 (2000).
4. C.K. Hitzenberger, A. Baumgartner, A.F. Fercher, „Dispersion induced multiple signal peak splitting in partial coherence interferometry," Opt. Commun. **154**, 179-185 (1998).
5. W. Drexler, U. Morgner, F.X. Kärtner, C. Pitris, S. A. Boppart, X.D. Li, E.P. Ippen, J.G. Fujimoto, „In vivo ultra-high resolution optical coherence tomography," Opt. Lett. **24**, 1221-1223 (1999).
6. A.F. Fercher, C.K. Hitzenberger, M. Sticker, R. Zawadzki, B. Karamata, T. Lasser, "A new dispersion compensation technique for Partial Coherence Interferometry (PCI) and Optical Coherence Tomography (OCT)," Proc SPIE **4431** (to be published).
7. A. Ghatak and K. Thyagarajan, *Introduction to Fiber Optics* (Cambridge University Press, 1998).
8. C.K. Hitzenberger, A. Baumgartner, W. Drexler, A.F. Fercher, "Dispersion effects in partial coherence interferometry: implications for intraocular ranging," J. Biomed. Opt. **4**, 144-151, 1999.
9. M. Born and E. Wolf, *Principles of Optics* (Cambridge University Press, 1998).
10. A.-G. Van Engen, S. Diddams, T.-S. Clement, "Dispersion measurements of water with white-light interferometry," Appl. Opt. **37**, 5679-5686, 1998.
11. T. Fuji, M. Miyata, S. Kawato, T. Hattori, H. Nakatsuka, "Linear propagation of light investigated with a white-light Michelson interferometer", J. Opt. Soc. Am. **B 14** 1074-1078, 1997.
12. SCHOTT'96 for Windows Catalog Optical Glass, Schott Glaswerke Mainz, Germany, 1996, <http://us.schott.com/sgt/english/products/catalogs.html>.
13. J.M. Schmitt and G. Kumar, "Optical scattering properties of soft tissue: a discrete particle model," Appl. Opt. **37**, 2788-2797, 1998.

## 1. Introduction

Partial coherence interferometry (PCI) [1] and optical coherence tomography (OCT) [2] have found many applications for high precision non-contact ranging and imaging in technical and medical fields. In both cases depth positions of light remitting sites in objects are measured by the so-called depth scan using back scattered light in a partial coherence interferometer.

The recent use of broadband light sources has dramatically increased depth resolution in PCI and OCT. Besides the space coherence problem introduced by some of these light sources [3], increasing the bandwidth increases dispersion related loss of depth resolution [4]. Hence, dispersion must carefully be compensated for in ultrahigh resolution OCT; usually some additional dispersing material is physically introduced into the reference arm of the interferometer [5]. This paper presents a numerical solution for compensation of dispersion related loss of depth resolution in PCI and OCT [6].

## 2. Dispersion in PCI and OCT

Dispersion has several consequences for PCI and OCT:

(1) PCI ranging and OCT imaging rely on matching path lengths for wave groups. Therefore, depth resolution is related to the coherence length  $l_c$  of the light used in the depth scan. If the light source has a Gaussian emission spectrum the coherence length is

$$l_c = \frac{4 \ln 2}{\pi} \frac{\lambda_0^2}{\Delta \lambda} \quad (1)$$

where  $\lambda_0$  is the center wavelength and  $\Delta \lambda$  is the FWHM spectral width of the emitted light. In PCI ranging and OCT imaging the optical distances are determined by the group index  $n_g$  rather than the phase index  $n$ , used in classical interferometry. Furthermore, back-reflected light is used, hence, depth resolution is  $\Delta z = l_c / 2n_g$ .

The group index  $n_g$  includes the phase index  $n$  and the phase index dispersion by

$$n_g = c \frac{dk}{d\omega} = n - \lambda \frac{dn}{d\lambda}. \quad (2)$$

Therefore, depth resolution improves with first-order dispersion  $\frac{dk}{d\omega}$ .

(2) Optically, materials are characterized by a nonvanishing second-order dispersion or group dispersion:

$$\frac{dn_g}{d\lambda} = -\lambda \frac{d^2 n}{d\lambda^2} = -\lambda \frac{2\pi\nu^3}{c} \frac{d^2 k}{d\omega^2} \quad (3)$$

$\nu$  is the light frequency. Group dispersion increases coherence length. For example, a Fourier transform limited Gaussian pulse the temporal  $1/e$ -width  $\tau_0$  is extended by a factor  $f$  [7]:

$$f = \sqrt{1 + \frac{4d^2}{\tau_0^4} \left( \frac{d^2 k}{d\omega^2} \right)^2}, \quad (4)$$

$d$  is the distance travelled by the wave in the dispersive material. Low coherence light can be considered as a random temporal distribution of ultrashort Fourier transform limited Gaussian pulses [7], hence, the dispersed coherence length of low coherence light is of the order of

$$I_{C,dispersed} = I_C \cdot f \quad (5)$$

i. e. depth resolution of PCI ranging and OCT imaging is degraded by a factor  $f$ .

(3) Because of energy conservation of the light pulses a reduction of the pulse intensity occurs even in non-absorbing media. Therefore, for a random temporal distribution of ultrashort Fourier transform limited Gaussian pulses the maximum fringe visibility as well as the PCI and OCT signal amplitude are reduced and the signal to noise ratio is decreased by a factor of  $\sqrt{f}$  [7].

(4) Furthermore, dispersion gives rise to artifacts. For example, it has been shown, that a beat effect occurs if a thin object behind a dispersive medium is to be measured by PCI or imaged by OCT [4].

### 3. Dispersed Light Waves

Light waves exiting from the interferometer exhibit path dependent phase changes in their spectrum. This can be seen from the Fourier shift theorem and the fact, that the spectral density  $G(\omega)$  and the real coherence function  $G(\tau)$  form a Fourier transform pair [9]:

$$G(\tau) = \langle E(t) \cdot E(t + \tau) \rangle = \int_{-\infty}^{\infty} G(\omega) e^{-i\omega\tau} d\omega ; \quad (5)$$

$E(t)$  is the electric field component of the light wave. A time delay  $\tau_0$  in the coherence function, as it occurs in the depth scan, leads to a phase  $\Phi_0 = \omega\tau_0$ , linear in  $\omega$ , in the spectral density:

$$G(\tau + \tau_0) = \int_{-\infty}^{\infty} G(\omega) e^{-i\Phi_0} e^{-i\omega\tau} d\omega \quad (6)$$

Propagation in a dispersive medium adds an additional phase  $\Phi_{Disp}(\omega)$  depending on the properties of the dispersive sample:

$$G_{Disp}(\tau + \tau_0) = \int_{-\infty}^{\infty} G(\omega) e^{-i(\Phi_0 + \Phi_{Disp})} e^{-i\omega\tau} d\omega . \quad (7)$$

$\Phi_{Disp}(\omega)$  can be developed into a Taylor series [10]:

$$\begin{aligned} \Phi_{Disp}(\omega - \omega_0) &= k(\omega - \omega_0)z \\ &= k(\omega_0)z + k^{(1)}(\omega_0)(\omega - \omega_0)z + k^{(2)}(\omega_0)\frac{(\omega - \omega_0)^2}{2}z + k^{(3)}(\omega_0)\frac{(\omega - \omega_0)^3}{6}z + \dots \end{aligned} \quad (8)$$

with  $k^{(j)}(\omega_0) = \left( \frac{d^j k}{d\omega^j} \right)_{\omega=\omega_0}$  being the  $j^{\text{th}}$  order dispersion;  $z$  is the path length in the dispersive medium.

First order dispersion  $k^{(1)}(\omega_0)$  adds a phase term linear in  $\omega$  to the intensity spectrum. It determines the group velocity [9]:

$$v_g = \left[ k^{(1)}(\omega_0) \right]^{-1} \quad (9)$$

Second and higher order dispersion terms add a phase nonlinear in  $\omega$  and, therefore, increase the coherence length.

The impact of any sample on the probe light wave in an interferometer can be shown to be reflected by the change of the auto-correlation signal at the interferometer exit to the cross-correlation signal [11]. Let us represent  $E(t)$  as a Fourier integral:

$$E(t) = \int_{-\infty}^{\infty} \hat{E}(\omega) e^{-i\omega t} d\omega, \quad (10)$$

then the interference term at the exit of an interferometer is the auto-correlation [9]:

$$I_{IT}(\tau) = G(\tau) = \langle E(t+\tau)E^*(t) \rangle = \int_{-\infty}^{\infty} d\omega G(\omega) e^{-i\omega\tau} \quad (11)$$

A dispersing sample in the interferometer will introduce phases  $\Phi_{Disp}(\omega)$  to the spectral components of the light in the probe beam. Introducing  $\Phi_{Disp}(\omega)$  to the phases of the waves in equation (11) yields the cross-correlation:

$$I_{IT}(\tau) = \langle E(t+\tau)E^*_{Disp}(t) \rangle = \int_{-\infty}^{\infty} d\omega G(\omega) e^{-i\omega\tau} e^{-i\Phi_{Disp}(\omega)}. \quad (12)$$

Hence, the intensity  $I_{IT}(\tau)$  at the interferometer exit with dispersion in the sample arm equals the Fourier transform of the spectral intensity  $G(\omega)$  at the interferometer exit without dispersion multiplied by the dispersion phase coefficient  $e^{-i\Phi_{Disp}(\omega)}$ .

Therefore, the impact of dispersion can be neutralized in two ways: in the standard balancing technique a dispersive plate is introduced into the reference arm of the interferometer which provides the same dispersion as the sample. Alternatively, dispersion can be compensated numerically by compensating the dispersion phase coefficient in the interferometer exit signal.

#### 4. Numerical Dispersion Compensation

Numerical dispersion compensation can either be performed in direct space or in Fourier space. In Fourier space the local Fourier components of the interferometer exit signal have to be multiplied by the complex conjugate of the dispersion phase coefficient:

$$I_{Comp}(\tau) = FT \{ I_{local}(\omega) \exp(i\Phi_{local}(\omega)) \}. \quad (13)$$

A windowed Fourier transform or a wavelet transform can be used and the window width will depend on the acceptable amount of residual dispersion. Within each window the transform of the interferometer exit signal has to be multiplied by the complex conjugate of the local dispersion phase coefficient  $\exp(i\Phi_{local}(\omega))$ .

In the example shown in figure 1 a correlation technique is used. Here the depth scan signal is correlated with a depth dependent kernel  $K_{local}(\tau)$ :

$$I_{Comp}(\tau) = I_{local}(\tau) \otimes K_{local}(\tau) \quad (14)$$

$I_{local}(\tau)$  is the local interference term.  $K_{local}(\tau)$  is the response of a light remitting site at depth  $z$ , subject to the dispersion at position  $z$  or the corresponding time delay  $\tau$  with respect to the reference beam. The (undispersed) kernel at the surface of the dispersing object is the auto-correlation of the light wave exiting the source. This can be obtained from the light source data using standard textbook formulas. In most cases the spectrum can be approximated by a Gaussian and, therefore, the undispersed kernel too can be approximated by a Gaussian temporal distribution:

$$K(t) = ae^{-t^2/\tau_0^2} e^{i\omega_0 t} . \quad (15)$$

The depth dependent local kernel  $K_{local}(\tau)$  is obtained from the undispersed kernel  $K(t)$  by adding a depth dependent phase nonlinear in  $\omega$  caused by the second and higher order dispersion terms to the Fourier components  $\hat{E}(\omega)$ . This phase leads to a broadening of the light pulses and, therefore, generates chirping of these pulses: their instantaneous frequency changes with time [7]. The local kernel  $K_{local}(\tau)$  equals the cross-correlation signal of the interferometer and, therefore, its FWHM duration increases with increasing coherence length of the light remitted at the corresponding object depth.

Figure 1 presents an example of the correlation technique. A Michelson bulk optics interferometer has been used; the light source was a Hg high pressure lamp. Light from this lamp was filtered by a Schott OG590 filter. We have duplicated the depth scan signal of a microscope cover glass (BK7, 144  $\mu m$  thick) to demonstrate the power of this technique: Two non-dispersed front signals and two dispersed back signals were mathematically added with a mutual shift of 2,5  $\mu m$ . In fact this is an indirect proof but based on experimental data. To provide a reasonable picture most of the data between the two interfaces have been omitted. The undispersed Gaussian kernel was based on a mean wavelength of  $\lambda_0 = 710 nm$  and  $\tau_0 = 0,35 \cdot 10^{-14} s$ . Only second order dispersion has been compensated using a dispersed kernel based on 144  $\mu m$  path length in the dispersive medium.

The dispersion coefficient used in this work has been obtained from Sellmeier's formula and BK7 refractive index data out of Schott Catalog Optical Glass [12]:

$$n(\lambda) = \sqrt{1 + B_1 \frac{\lambda^2}{\lambda^2 - C_1} + B_2 \frac{\lambda^2}{\lambda^2 - C_2} + B_3 \frac{\lambda^2}{\lambda^2 - C_3}} \quad (16)$$

with constants  $B_1 = 1.03961212$ ;  $B_2 = 0.231792344$ ;  $B_3 = 1.01046945$ ;  $C_1 = 0.00600069867$ ;  $C_2 = 0.0200179144$ ;  $C_3 = 103.560653$ . Using equation (16) a significant variation of the second order dispersion within the broad bandwidth of the light used in our experiment is found. We used a mean value of  $\frac{d^2 n}{d\lambda^2} = 0.085 \mu m^{-2}$  corresponding to the center wavelength of  $\lambda_0 = 710 nm$ .

Furthermore, we approximated the filtered Hg-spectrum by a Gaussian distribution. Though the filtered spectrum does more resemble a skewed Gaussian distribution this approximation worked quite well. Hence we feel, that the detailed structure of the spectrum is of minor importance; it is the chirping determined by the wavelength bandwidth and the probe depth which provide the basis for reducing the correlation width.

Whereas the direct signal in figure 1 does not resolve the 2,5  $\mu m$  distance of two back interfaces the numerical correlation shows a pronounced dip between the two correlation peaks. The shift of the numerical correlation peaks to the left is the width of the correlation kernel. It has not been removed to ease comparison. The amplitude of the dispersed depth scan

signal (right) has been increased mathematically to ease the comparison with the non-dispersed depth scan signal.

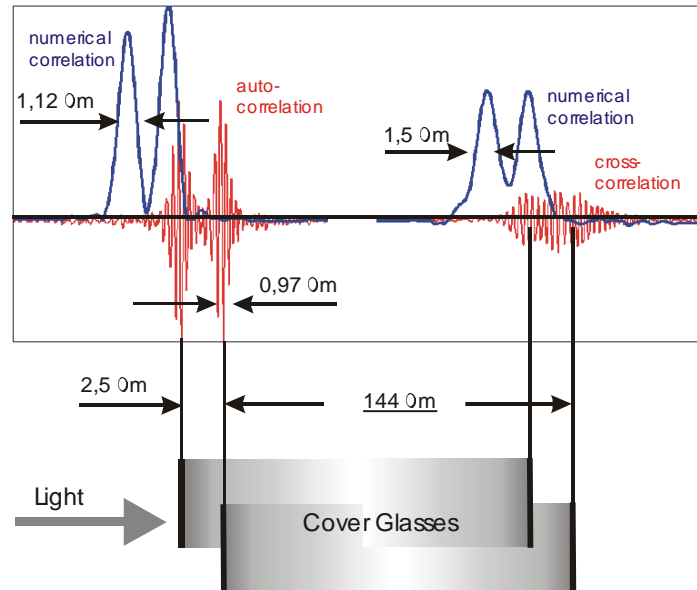


**Fig. 1:** Resolution improvement obtained by dispersion compensation using depth-variant numerical correlation. Light of a filtered Hg high pressure lamp ( $\lambda_0 \cong 710 \text{ nm}$ ;  $\Delta\lambda \cong 210 \text{ nm}$ ) is incident from left (thick arrow). The object has been synthesized using experimentally obtained non-dispersed front and dispersed back scattered depth scan signals of a single microscope cover slide. Shown are the (direct) auto- and cross-correlation depth scan signals (red) of the two front and the two back interfaces and the corresponding numerically dispersion-compensated correlation signals (black).

## 5. Conclusions

In this report we describe a numerical correlation technique to compensate depth resolution loss caused by dispersion in partial coherence interferometry and optical coherence tomography. This technique can be used *a posteriori* and can easily realize a dynamic dispersion scheme. Dispersion compensation is achieved by correlating the depth scan signal with a depth-dependent correlation kernel.

When scanning materials with unknown refraction properties, the depth scan signal from a single back scattering interface within the object or from the back surface of the object can be used as an empirical basis for the correlation kernel. This can also be done *a posteriori*. Biological tissue contains about 70 % water and 30 % mainly proteins. Hence dispersion properties of such tissue are mainly determined by these components. For a first approximation water data might be used which are easily available [10]. A recent collection of published optical properties of tissues can be found in Reference [13]. However, these data do not suffice to derive higher order dispersion figures. So far we have not yet found higher order dispersion data of proteins. But here too one might use the depth scan signal obtained from a single back scattering interface within the object or from the object back surface as an empirical basis for the correlation kernel.

**Acknowledgement.** Financial support from the Austrian *Fonds zur Förderung der Wissenschaftlichen Forschung* (Project No. 10316) and from the *Jubiläumsfonds* (Project No. 7428) of the Austrian National Bank is acknowledged.